Journal of Solid State Chemistry 182 (2009) 2549–2554

Contents lists available at ScienceDirect

Journal of Solid State Chemistry

journal homepage: www.elsevier.com/locate/jssc

Neutron diffraction study of the β' and γ phases of $LiFeO_2$

Maud Barré, Michele Catti *

Dipartimento di Scienza dei Materiali, Università di Milano Bicocca, via Cozzi 53, 20125 Milano, Italy

ARTICLE INFO

Article history:
Received 29 April 2009
Received in revised form
15 June 2009
Accepted 19 June 2009
Available online 24 June 2009

Keywords:
Neutron diffraction
$LiFeO_2$
Lithium ion materials
Order–disorder phase transitions

ABSTRACT

The β, β', γ and α phases of $LiFeO_2$, synthesized as powders, were annealed at different temperatures and characterized by X-ray measurements. The β' and γ modifications were also studied by time-of-flight neutron diffraction (ISIS Facility, UK). The structure of the β' phase was refined in the monoclinic $C2/c$ space group ($a = 8.566(1)$, $b = 11.574(2)$, $c = 5.1970(5)$ Å, $\beta = 146.064(5)^\circ$) to w$R_p = 0.071$–0.080 (data from four counter banks). Fe and Li atoms are ordered over two of the four independent sites, and partially disordered over the other two. The ordered Li has a distorted tetrahedral coordination. The γ structure was refined at RT ($a = 4.047(1)$, $c = 8.746(2)$ Å) and at 570 °C ($a = 4.082(3)$, $c = 8.822(6)$ Å) in the $I4_1/amd$ symmetry, showing full order with Li in octahedral coordination at RT, and in a split-atom configuration at high temperature. On annealing, the β' polymorph was found to transform to γ at 550 °C, thus suggesting that it is a metastable phase. Electrostatics is discussed as the driving force for the $\alpha \rightarrow \beta' \rightarrow \gamma$ ordering process of $LiFeO_2$.

1. Introduction

The $LiMO_2$ oxides are well known for their applications as cathode materials in 'rocking-chair' lithium batteries. In particular, a $LiCoO_2$ cathode coupled to a Li-intercalated graphite anode makes up the most widespread rechargeable battery for portable phones and computers. Several *M* transition metals were thoroughly tested, in the search for cheaper and more environment-friendly than cobalt alternatives. In particular, $LiFeO_2$ shows an amazingly complex polymorphism, and its electrochemical activity seems to depend strongly on the crystalline modification [1,2]. At least nine different polymorphs are reported to be stable or metastable at room temperature for $LiFeO_2$. The first group is formed by the cubic disordered rocksalt-type α phase, and by its β (tetragonal), β' (reported as monoclinic, orthorhombic or tetragonal), β'' (tetragonal) and γ (tetragonal) superstructures [3]. Then a rhombohedral ordered rocksalt superstructure analogous to $LiCoO_2$ [4,5], a hollandite-type tetragonal phase [2], and two orthorhombic phases isostructural with $LiMnO_2$ [1] and with β-$NaFeO_2$ [6], respectively, were described. Yet complete structure determinations of many of these phases are missing.

The focus of this paper is on the first group of polymorphs: therein only X-ray powder diffraction refinements were reported for the α and β modifications [7,8], and an old neutron diffraction study for the γ phase [9]. Further, the β and β' phases are often confused with each other: cf. the calorimetric study of the relative stabilities of the α, β and γ polymorphs, where the β-named modification is actually β' by inspection of the reported X-ray patterns [10]. The magnetic properties of these materials, including antiferromagnetic ordering, were investigated as well [9,11].

A careful study of the detailed structural features of these phases is important for several reasons. First, it is necessary to detect the real location of Li atoms inside their structures, to explain why some of them are electrochemically active and others are not. Indeed, there are good grounds to believe that in many of these cases the Li atom may actually be in tetrahedral rather than in octahedral coordination, as proved in previous investigations of perovskite-type lithium conductors (LLTO phases) [12]. The coordination environment and order–disorder state of lithium is relevant to assess the ion mobility paths and transport mechanisms inside the crystal structure. In this respect, one of the open structural issues with this system is that of the Fe^{3+}/Li^+ disordered distribution, which should be quite unfavoured (except possibly for the high temperature α phase) by the large charge unbalance between the two ions. Further, the phase transformations among the different polymorphs on heating should be elucidated from the point of view of the related detailed structural changes, in order to understand what may happen in electrochemical devices at variable temperatures. Thus, a thorough structural characterization by NPD is needed for the $LiFeO_2$ phases.

In the frame of a long-term research activity on Li^+ ion conductors, the synthesis and structural study of the α, β, β' and γ polymorphs of lithium iron oxide by neutron powder diffraction were undertaken. Here the results concerning the β' and γ phases are presented in detail.

* Corresponding author. Fax: +39 02 64485400.
E-mail address: catti@mater.unimib.it (M. Catti).

0022-4596/$ - see front matter © 2009 Elsevier Inc. All rights reserved.
doi:10.1016/j.jssc.2009.06.029

2. Experimental

2.1. Synthesis

Following previous results from the literature, the β phase of $LiFeO_2$ was prepared by hydrothermal synthesis at 200 °C for 48 h, in a Teflon-lined autoclave, starting from a $FeCl_3$ water solution to which LiOH had been added in a 10:1 ratio with respect to stoichiometry [3]. The products were then filtrated and washed repeatedly with distilled water to remove the excess of LiOH. Finally, the obtained powder was dried at 100 °C for 10 h.

The α and γ varieties of $LiFeO_2$ were both synthesized by solid state reaction from stoichiometric amounts of Fe_2O_3 and Li_2CO_3 [7,13]. These compounds were ground and heated in a furnace at 700 °C for 12 h, and at 600 °C for 60 h to obtain the α and γ phases, respectively. The β' variety was synthesized by annealing α-$LiFeO_2$ at 400 °C for 150 h. It should be noticed that, on annealing α-$LiFeO_2$ at a lower temperature, the β' rather than β phase (as previously reported [7]) was still obtained.

A Pechini-type complex polymerizable method was also attempted to synthesize these materials, starting from stoichiometric amounts of Li_2CO_3 and Fe_2O_3 dissolved in nitric acid. The reagent ions were complexed by citric acid (CA) and then polyesterified at 100 °C with ethylene glycol (EG) (molar ratio CA/EG:1/4). The reaction produced a gel which was dried at 150 °C and then heated in a furnace at 400 °C for 12 h to obtain the precursor powder. The β, γ and α phases were formed after annealing the precursor at 400, 600 and 700 °C, respectively. However, the samples obtained had a worse crystal quality than those prepared by hydrothermal and solid state methods, which were then subsequently used for the present study.

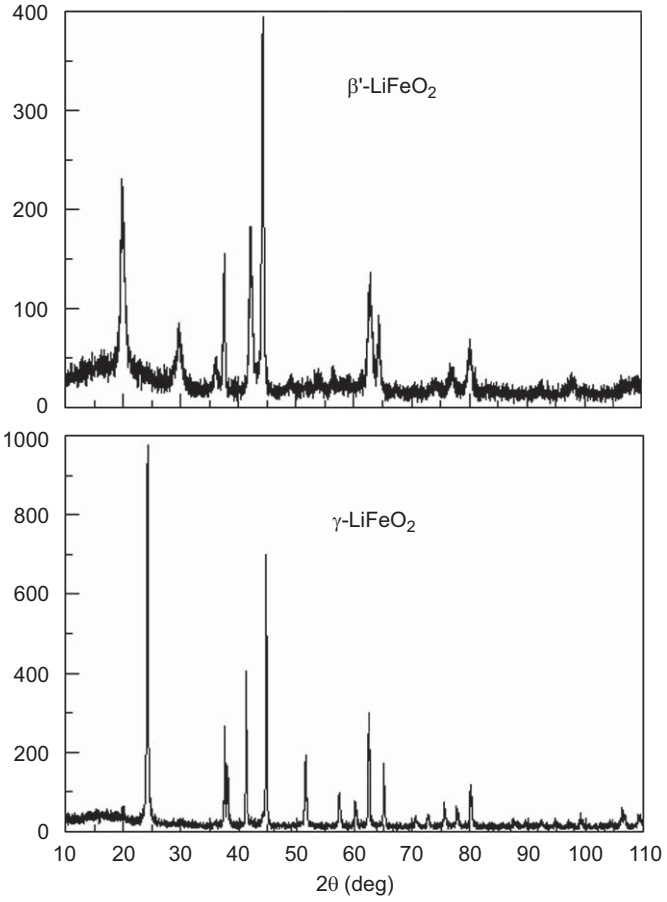

Fig. 1. X-ray diffraction patterns (Cu$K\alpha$ radiation) of the β' and γ phases of $LiFeO_2$.

2.2. X-ray diffraction and ex-situ thermal study

X-ray powder diffraction patterns were collected on all samples by a Bruker D8 Advance diffractometer (Cu$K\alpha$ radiation) with θ/θ geometry and secondary beam monochromator (2θ step = 0.02°, step time = 12 s). The previously reported unit cells were confirmed for all phases, obtaining: $a = 2.894(3)$ and $c = 4.282(4)$ Å (I lattice) for β, $a = 4.0466(1)$ and $c = 8.7467(2)$ Å (I lattice) for γ and $a = 4.152(1)$ Å (F lattice) for α. In the case of the β' modification, both a C monoclinic ($a = 8.565(5)$, $b = 11.553(7)$, $c = 5.188(3)$ Å, $\beta = 146.10(1)°$) and a I tetragonal ($a = 11.586(6)$, $c = 8.581(5)$ Å) cell fitted the diffraction pattern. The crystal quality of samples α and γ was very good, whereas Bragg peaks became broader for the β' and very broad for the β sample. The patterns obtained for the β' and γ phases are shown in Fig. 1.

The phase transformations between the β–β', γ and α phases of $LiFeO_2$ were studied by two series of experiments. First, an α sample was annealed in steps of 1 h, each followed by cooling and *ex-situ* X-ray diffraction at RT, with 10 °C (in the 440–600 °C range) and 20 °C (600–740 °C) intervals. Second, a β sample was similarly annealed with 20 °C intervals in the 400–700 °C range.

2.3. Neutron diffraction measurements

Data were collected on samples of the β' and γ phases of $LiFeO_2$ by the INES time-of-flight diffractometer at the ISIS pulsed spallation source (Rutherford Appleton Laboratory, Chilton, Didcot, UK). Two powder specimens of about 2 cm^3, put in vanadium cans under vacuum, were employed. For each sample, intensity profiles were measured by use of nine counter banks located at 2θ ranging from 162.83° to 19.07°. The corresponding $\Delta d/d$ resolution range is 0.0012–0.013. Data recorded on the four high-angle banks ($2\theta = 162.83$–$109.07°$, $d_{hkl} = 0.319$–1.985 Å) were used for the Rietveld refinements. Patterns collected on the lower resolution counter banks were taken into account for indexing and preliminary unit-cell determination. The experiments at room temperature lasted 10 and 8 h for the β' and γ phases, respectively. Some measurements were also performed with a resistance furnace surrounding the can. A long run (12 h) was carried out at 570 °C for the structural study of the γ phase just above the β' to γ transition, and shorter runs (1–2 h) at 300, 400, 500, 550 and 650 °C.

Preliminary data reductions were performed, including merging of outputs from single counters in the bank and correction for detector efficiency as a function of neutron wavelength. The Rietveld refinements of the crystal structures were carried out by the FULLPROF computer package [14]. The intensity background was fixed by selected points, and the peak shape was represented by a convolution of a pseudo-Voigt function (linear combination of Gaussian and Lorentzian components, with σ and γ half-widths, respectively: sample contribution) with two back-to-back exponentials (instrumental and moderator contributions) [15]. The σ and γ parameters were assumed to depend on d_{hkl} according to $\sigma = (\sigma_1 d_{hkl}{}^2 + \sigma_2 d_{hkl}{}^4)^{1/2}$ and $\gamma = \gamma_1 d_{hkl} + \gamma_2 d_{hkl}{}^2$, where the σ_1, σ_2, γ_1, γ_2 quantities were included in the refinement. The mixing coefficient and the full width of the pseudo-Voigt function depend on σ and γ according to equations given in the literature [16].

3. Results and discussion

3.1. Crystal structure of β'-$LiFeO_2$ at RT

On the basis of the X-ray powder diffraction pattern, the β' phase of $LiFeO_2$ was reported to be either monoclinic $C2/c$ or

face-centred orthorhombic (with unspecified space group) [3], but without solving or refining its structure. In order to interpret precession photographs of a twinned single crystal sample, two ordered (monoclinic $C2/c$ and tetragonal $I4_1/amd$) structural models were proposed, corresponding to superstructures of the rocksalt-type α phase [8]. In both cases, O atoms are in the ideal FCC arrangement and four independent cation sites in the octahedral holes are occupied by two Fe and two Li atoms. The orthorhombic hypothesis is found to be inconsistent with both models. Although an F cell with right angles can be obtained from the monoclinic one by the [010/102/100] transformation, no F-type orthorhombic space group can fit with the $C2/c$ structural arrangement. On the other hand, the ordered $C2/c$ monoclinic model proved to be a good starting point for Rietveld refinement.

After the first cycles, both Fe and Li were put on each of the four cation sites and their occupation factors were let to vary, with the constraints of full site occupation and of the overall $LiFeO_2$ stoichiometry. Two of them confirmed to be pure Fe and Li sites, respectively, but the other two showed a mixed composition with prevalence of Fe or of Li. As the shortest Li–O distance obtained (1.77 Å) was considered to be too small, a restraint was introduced in the refinement, fixing the minimum value to 1.80 Å. The last cycle converged to the agreement factors given in Table 1, where also the unit-cell constants, the number of data from the four counter banks, and the number of refined structural+profile parameters are reported. In Fig. 2, the measured, calculated and difference profiles are shown for data collected on the bank at $2\theta = 109.07^\circ$. The refined fractional atomic coordinates, occupancies and displacement factors are given in Table 2. The e.s.d.'s of the coordinates appear to be larger than usual, and this is due mainly to the broadness of the Bragg peaks.

The most important structural features of the monoclinic β' structure are as follows: first, only two out of four independent cation sites (Fe3 and Li3) are fully ordered, whereas the other two show partially disordered $Fe_{0.56}Li_{0.44}$ and $Li_{0.56}Fe_{0.44}$ compositions. Of course fully ordered models could be devised by lowering the symmetry to subgroups of $C2/c$. As there are no indications of the presence of superlattice reflections, the current unit cell must be kept anyway. In the monoclinic subgroup $C2$ the number of independent cation sites is doubled, whereas in Cc it is not. We tried to refine the $C2$ ordered models, but divergence occurred. The refinement of the crystal structure in the Cc space group was also attempted and it did converge, but giving a semi-disordered distribution of Fe/Li over the four sites similar to that observed in $C2/c$, and with e.s.d's of the coordinates about 10 times larger.

Second, the largest distortions with respect to the ideal FCC atomic coordinates are observed for Li3 ($y = 0.850$ vs. 0.8125) and for O1 and O2 ($z = 0.265$ and 0.267, respectively, vs. 0.25). The main result is that Li3 moves off the centre of the octahedron along y, approaching the O1–O1′ edge so as to attain a distorted tetrahedral environment (Fig. 3): the Li3–O1 and Li3–O1′ bond distances are very short, but the other two are much longer (Table 3). If the next longer contacts of 2.41 Å are still considered to be appreciably bonding, the coordination number can indeed be considered to be 4+2. Indeed, by taking the sums of Li^+ and O^{2-} ionic radii according to Shannon and Prewitt [17], one obtains 1.99 and 2.16 Å for the expected bond distances of four-fold and six-fold coordinated lithium, respectively, to six-fold coordinated oxygen. This agrees satisfactorily with the average Li3–O distances reported for both cases in Table 3.

As for bond distances in the pure Fe3 coordination octahedra, the average value corresponds to the expected distance (2.045 Å) on the basis of ionic radii. This is also the case for the 'mixed' Fe1/Li1 octahedron, where the site composition is actually richer in Fe. We observe instead a substantially longer average bond distance in the Li-richer Li2/Fe2 octahedron, consistently again with the expected value of 2.16 Å quoted above for the Li–O distance.

As the β' phase is a partially ordered superstructure of the rocksalt-type α modification, it is interesting to examine the β'–α relationships. The $C2/c$ unit cell vectors of β' can be obtained by the $Fm\bar{3}m$ ones of α according to the $[2\,0\,0/0\,2\,-2/\,-1\,\frac{1}{2}\,\frac{1}{2}]$ transformation matrix. It follows that the close-packed atomic layers have (100) orientation in the monoclinic reference (cf. Fig. 3), and the cations are arranged as partially ordered sequences of

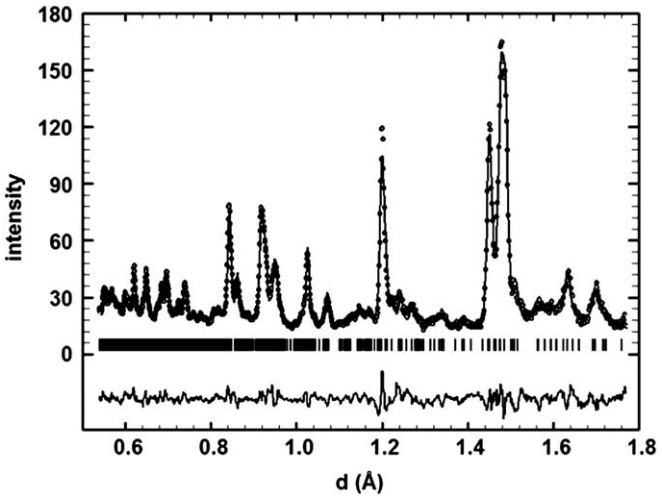

Fig. 2. Time-of-flight neutron diffraction pattern of β'-$LiFeO_2$, recorded on the counter bank at $2\theta = 109.07^\circ$. Experimental (circles), calculated and difference profiles are shown.

Table 1
Unit-cell constants (with e.s.d.'s in parentheses), agreement indexes (range over four counter banks) and other details of the Rietveld refinements of the β' and γ phases of $LiFeO_2$ from neutron powder diffraction measurements.

	β'	γ	γ
T (°C)	25	25	570
a (Å)	8.566(1)	4.047(1)	4.082(3)
b (Å)	11.574(2)	4.047(1)	4.082(3)
c (Å)	5.1970(7)	8.746(2)	8.822(6)
β (deg)	146.064(5)	90	90
V (Å^3)	287.65	143.27	147.00
Data	6530 (4 banks)	6530 (4 banks)	6530 (4 banks)
Variables	21+16	6+24	7+24
R_p	0.060–0.070	0.063–0.074	0.035–0.044
wR_p	0.071–0.086	0.066–0.083	0.054–0.065
$R(F^2)$	0.069–0.086	0.062–0.066	0.066–0.100

Table 2
Atomic fractional coordinates, site occupancies and isotropic displacement factors of room temperature β'-$LiFeO_2$ ($C2/c$ space group, $Z = 8$) from NPD Rietveld refinement.

	Site	s.o.f.	x	y	z	B (10^{-2} Å^2)
Fe1	4*e*	0.56(2)	0	0.063(3)	0.25	0.1(3)
Li1		0.44(2)				
Fe2	4*e*	0.44(2)	0	0.562(6)	0.25	0.8(7)
Li2		0.56(2)				
Fe3	4*e*	1	0	0.313(2)	0.25	1.5(2)
Li3	4*e*	1	0	0.850(1)	0.25	0.2(5)
O1	8*f*	1	0.244(2)	0.064(1)	0.265(4)	0.3(2)
O2	8*f*	1	0.249(2)	0.312(3)	0.267(3)	0.3(2)

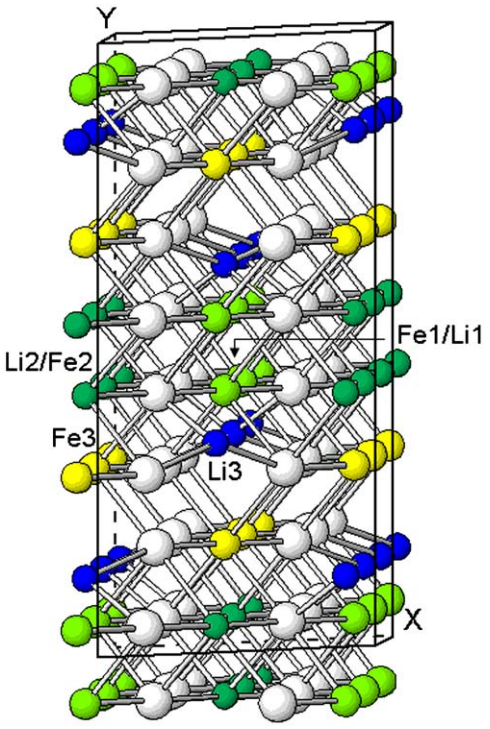

Fig. 3. View along [001] of the crystal structure of monoclinic β'-$LiFeO_2$. Pale grey, black (colour online: yellow, blue) and white spheres represent Fe, Li and O atoms, respectively. Sites with disordered cation distributions (dark grey balls, colour on line: green) are denoted as Fe1/Li1 and Li2/Fe2. (For interpretation of the references to colour in this figure legend, the reader is referred to the web version of this article.)

Table 3
Interatomic Fe–O and Li–O distances (Å) of β'-$LiFeO_2$.

Fe1/Li1–O1	2.03(2) × 2
Fe1/Li1–O1′	2.10(4) × 2
Fe1/Li1–O2	2.02(4) × 2
⟨Fe1/Li1–O⟩	2.05
Li2/Fe2–O1	2.26(2) × 2
Li2/Fe2–O1′	2.03(5) × 2
Li2/Fe2–O2	2.09(5) × 2
⟨Li2/Fe2–O⟩	2.13
Fe3–O1	2.00(2) × 2
Fe3–O2	2.02(3) × 2
Fe3–O2′	2.06(2) × 2
⟨Fe3–O⟩	2.03
Li3–O1	1.80(2) × 2
Li3–O2	2.27(2) × 2
Li3–O2′	2.41(3) × 2
⟨Li3–O⟩	2.03 ($CN = 4$)
	2.16 ($CN = 6$)

[001] rows within the (100) plane, according to the scheme Fe1/Li1, Fe1/Li1, Li3, Fe3, Li2/Fe2, Li2/Fe2, Li3, Fe3 in the [010] direction.

An attempt was also made to refine the β' structure according to the $I4_1/amd$ tetragonal model [8]; this should not be confused with the structure of the γ phase (cf. below), which accidentally shares the same space group. The transformation from the cubic $Fm\bar{3}m$ to the $I4_1/amd$ cell is [0−2−2/02−2/200], so that the tetragonal unit cell vectors are derived from the monoclinic ones according to the [−20−4/010/100] transformation. In order to comply with the orthogonal constraint of the tetragonal lattice, the monoclinic cell constants must satisfy the relation: $\cos\beta = -[(b/2a)^2+1]^{-1/2}$, which is indeed the case (Table 1). Convergence could be attained with the $I4_1/amd$ model ($a = 11.605(3)$, $c = 8.569(2)$ Å), but with values of the agreement indexes substantially worse than in the $C2/c$ case: $R_p = 0.097$–0.104, $wR_p = 0.121$–0.135, $R(F^2) = 0.102$–0.120 over the four counter banks (cf. Table 1). The occupancies of the four cation sites were quite similar, with two pure Fe and Li sites, and with a similar distorted environment of the latter Li atom, too. The monoclinic model is then considered to be more satisfactory than the tetragonal one.

3.2. Thermal study

The results of the *ex-situ* X-ray and *in-situ* neutron diffraction study vs. temperature are consistent. XRPD data show that, on heating, the α phase transforms to β' above 400 °C and remains associated to it up to 500 °C; then from 510 to 530 °C only β' is observed, from 540 to 580 °C β' coexists with γ, from 590 to 660 °C we have pure γ, in the range 680–700 °C the association γ+α is observed, and finally from 720 °C upwards only α is present. NPD results prove that, on heating, the β' phase remains pure to 500 °C, then at 550 °C it coexists with γ, at 570 °C only γ is observed, and at 650 °C the γ+α association is observed. Of course the *ex-situ* study shows slightly higher temperatures for the phase transitions, because of kinetic effects which the neutron *in-situ* results are free of. We can then conclude that the β' to γ transformation is first-order and occurs at 550 °C. The observed γ to α first-order transition at 650 °C confirms what reported previously [7,18].

The temperature dependence of the monoclinic lattice constants a, b and c of the β' phase is shown in Fig. 4. By least-squares linear interpolations, the following values are obtained for the coefficients of thermal expansions: 2.07×10^{-5} (a), 1.21×10^{-5} (b), 2.01×10^{-5} K^{-1}(c). A significant anisotropy is observed with the (010) plane parallel to the chains of Fe/Li octahedra expanding more than the normal direction (Fig. 3).

By the thermal study of the β phase, performed only by the *ex-situ* XRPD technique, the β to γ transition was found to occur in the range 500–550 °C, consistent with earlier results [7].

3.3. Structure of γ-$LiFeO_2$ at RT and high temperature

The Rietveld refinement of data collected at RT was started from the $I4_1/amd$ structural model of the previous neutron study [9], and convergence was reached with the unit-cell constants and

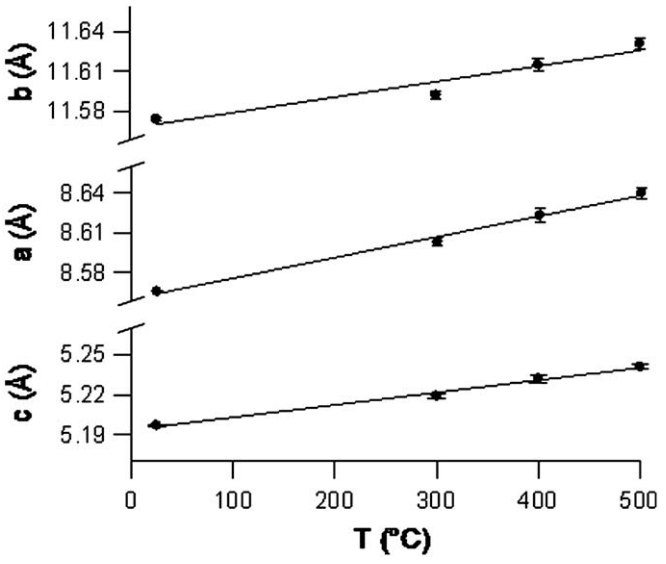

Fig. 4. Thermal expansion of the monoclinic unit-cell edges of β'-$LiFeO_2$ from NPD data.

Table 4
Atomic fractional coordinates, site occupancies and isotropic displacement factors of γ-$LiFeO_2$ ($I4_1/amd$ space group, origin choice 2, $Z=4$) from NPD Rietveld refinements at RT and just above the β' to γ phase transition.

	Site	s.o.f.	x	y	z	B (10^{-2} Å^2)
$T=25$ °C						
Fe	4*a*	1	0	0.75	0.125	0.39(4)
Li	4*b*	1	0	0.25	0.375	3.4(2)
O	8*e*	1	0	0.25	0.1068(2)	0.15(3)
$T=570$ °C						
Fe	4*a*	1	0	0.75	0.125	1.21(9)
Li	16*g*	0.25	0.066(3)	0.316(3)	0.375	6(1)
O	8*e*	1	0	0.25	0.1069(3)	0.45(5)

agreement factors reported in Table 1, and the atomic fractional coordinates of Table 4. The measured, calculated and difference profiles are shown in Fig. 5 for data recorded on the counter bank at $2\theta = 109.07°$. In the case of data measured at 570 °C, the Li atom in special position 4*b* showed a very large isotropic displacement factor of 13 Å^2. On employing anisotropic thermal motion, a revolution ellipsoid very flattened on the (001) plane was obtained. Then Li was displaced into the 16*g* position, according to a four-fold disordered split-atom model, and then convergence was attained with a quite reasonable isotropic displacement factor, less than twice the value obtained at RT (Table 4). However, two very short Li–O bond distances of 1.69 Å are found, so that a restraint was introduced in the refinement, fixing the minimum Li–O to be 1.80 Å. The final refined parameters with these conditions are reported in Tables 1 and 4. On attempting to refine Li disordered in the 32*i* general position, divergence occurred.

Pictures of the crystal structure of γ-$LiFeO_2$ at 25 and 570 °C are shown in Fig. 6, where the split-atom configuration of Li at high temperature appears clearly. On looking at the Li–O interatomic distances (Table 5), the LiO_6 coordination octahedron is noticed to be quite distorted already at RT, with elongation parallel to the *z* axis. This might have suggested a possible disorder of Li along *z* at high temperature, with passage from the 4*b* (0,1/4,3/8) to the 8*e* (0,1/4,*z*) Wyckoff position. Instead Li appears to move off the octahedron centre sideways to the 16*g* site (*x*,*x*+1/4,3/8). In this way two strong Li–O bonds are achieved, yet preserving weaker interactions with the other O atoms at corners of the octahedron.

3.4. Li/Fe ordering in the $\alpha \rightarrow \beta' \rightarrow \gamma$ phase transformations

The α, β' and γ modifications of $LiFeO_2$ are characterized by a complete disorder (α), partial disorder (β') and full order (γ) of the Li–Fe distribution in the octahedral sites of the basic rocksalt-type structure. This becomes more or less distorted, with a lowered symmetry, in the ordering process. However, an unusual thermal sequence of phase transformations is observed, as the intermediate β' phase is synthesized by annealing the α polymorph at a lower temperature than that necessary to obtain the full ordered γ phase; the latter one is also obtained by direct annealing of the β' modification. Ordering transformations induced by raising temperature are relatively uncommon, and usually relate metastable disordered phases to their stable ordered counterparts. This shows that the β' modification is not a thermodynamically stable phase, but a frozen intermediate stage of the ordering process transforming the α into the γ polymorph.

As the charge difference between Fe^{3+} and Li^+ is large, electrostatics is expected to be the main driving force for the ordering process. Pauling's rules [19] are a simple way to express

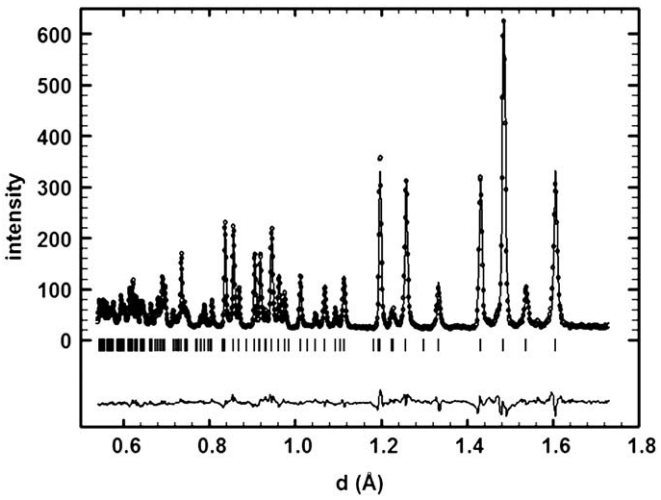

Fig. 5. Time-of-flight neutron diffraction pattern of γ-$LiFeO_2$ at room temperature, recorded on the counter bank at $2\theta = 109.07°$. Experimental (circles), calculated and difference profiles are shown.

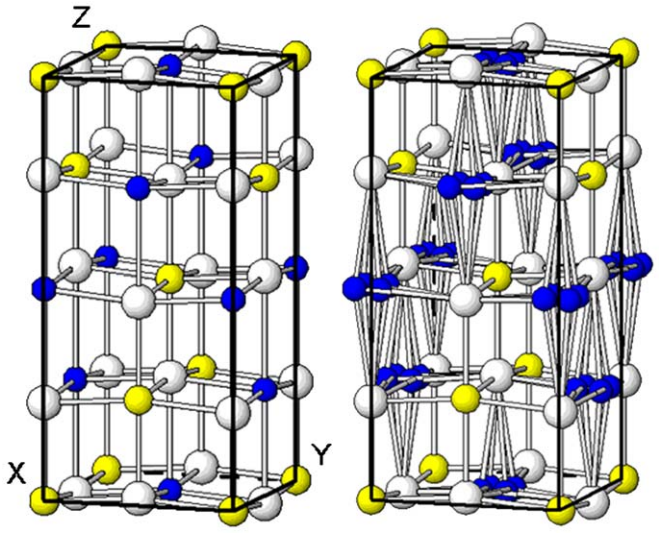

Fig. 6. Crystal structure of tetragonal γ-$LiFeO_2$ at 25 (left) and 570 °C (right), with origin choice 1 of $I4_1/amd$. Pale grey, black (colour online: yellow, blue) and white spheres represent Fe, Li and O atoms, respectively. The positional disorder of the Li atom at high temperature is emphasized. (For interpretation of the references to colour in this figure legend, the reader is referred to the web version of this article.)

Table 5
Interatomic Fe–O and Li–O distances (Å) of γ-$LiFeO_2$.

T	25	570 °C
Fe–O	2.0296(2) × 4	2.0472(2) × 4
Fe–O′	2.025(6) × 2	2.046(1) × 2
⟨Fe–O⟩	2.028	2.047
Li–O	2.0296(5) × 4	1.80(1) × 2
Li–O′		2.33(1) × 2
Li–O″	2.347(6) × 2	2.396(4) × 2
⟨Li–O⟩	2.135	2.175

the principle of minimum electrostatic energy in ionic crystals. According to the second rule, an O^{2-} ion receives a positive charge from each of the six surrounding cations which is equal to the

cation charge divided by six (cation coordination number). Their sum should be exactly 2, in order to compensate the anion charge. Let us consider the β' disordered structure as a mixture of two ordered configurations: S1 with pure Fe on site 1 and pure Li on site 2, and S2 with pure Li on site 1 and pure Fe on site 2 (cf. Table 2). If we compare the β'(S1), β'(S2) and γ configurations and compute the corresponding charge sums on the O atom, we obtain exactly 2 for both β'(S1) and γ, but 2.111 for β'(S2). Therefore, the β'(S2) configuration is electrically unbalanced and then energetically unfavoured with respect to β'(S1) and γ. This is consistent with the fact that, on the basis of refined occupancies (Table 2), the fraction of β'(S1) is slightly larger than that of β'(S2) in the disordered β' structure. Thus, an ordering transformation of the β' phase to either γ or a hypothetical ordered β'(S1) decreases the electrostatic energy of the system.

Why then only the first but not the second process is observed? To explain this, we should consider the first cation coordination sphere surrounding a given cation (say, a Fe^{3+} ion). This is made up by 12 cations at a distance of $a/\sqrt{2}$, which are partly Fe^{3+} and partly Li^{+}. The electrostatic repulsion with the central Fe^{3+} ion lowers as the fraction of Li^{+} cations in the coordination sphere increases. This fraction turns out to be 6/12, 7/12 and 8/12 in β'(S2), β'(S1) and γ, respectively. Therefore, the β'(S2) configuration is confirmed to be energetically unfavoured with respect to β'(S1), but in addition β'(S1) is shown to be less stable than γ. The ordering of β' to γ rather than to β'(S1) thus proves to be more convenient on electrostatic energy grounds.

4. Conclusions

The β' phase of $LiFeO_2$ was shown, by neutron diffraction measurements, to have a monoclinic $C2/c$ superstructure of the rocksalt-type α phase, which was successfully refined. The alternative tetragonal structure model gave a worse fit and was then discarded. Li and Fe atoms are fully ordered in two of the four independent cation sites, and partially disordered in the two other ones. On heating, β'-$LiFeO_2$ transforms into the $I4_1/amd$ ordered γ phase at 550 °C, according to a likely metastable character of the β' polymorph. This Li/Fe ordering process implies an electrostatic stabilization, because the number of Fe^{3+}–Li^{+} first neighbours increases with respect to those of Fe^{3+}–Fe^{3+} type, thus decreasing the cation–cation repulsion; further, the principle of local electroneutrality is better obeyed.

The coordination environment of lithium turns out to be tetrahedral distorted in the ordered site of the β' phase, octahedral in γ-$LiFeO_2$ at RT and split-disordered in the γ phase above the transition temperature. It is thus confirmed that the configuration of Li–O bonding is extremely sensitive to small chemical and thermal details of its surrounding structural framework.

Acknowledgments

We thank Antonella Scherillo for her help with the neutron diffraction measurements. The research was supported by a PRIN grant of MIUR, Rome (Cofin07 Project 200755ZKR3_004).

Appendix A. Supplementary material

Supplementary data associated with this article can be found in the online version at doi:10.1016/j.jssc.2009.06.029.

References

[1] R. Kanno, T. Shirane, Y. Kawamoto, Y. Takeda, M. Takano, M. Ohashi, Y. Yamaguchi, J. Electrochem. Soc. 143 (1996) 2435–2442.
[2] T. Matsumura, R. Kanno, Y. Inaba, Y. Kawamoto, M. Takano, J. Electrochem. Soc. 149 (2002) A1509–A1513.
[3] M. Tabuchi, K. Ado, H. Sakaebe, C. Masquelier, H. Kageyama, O. Nakamura, Solid State Ionics 79 (1995) 220–226.
[4] N. Douakha, M. Holzapfel, E. Chappel, G. Chouteau, L. Croguennec, A. Ott, B. Ouladdiaf, J. Solid State Chem. 163 (2002) 406–411.
[5] M. Tabuchi, K. Ado, H. Kobayashi, I. Matsubara, H. Kageyama, M. Wakita, S. Tsutsui, S. Nasu, Y. Takeda, C. Masquelier, A. Hirano, R. Kanno, J. Solid State Chem. 141 (1998) 554–561.
[6] A.R. Armstrong, D.W. Tee, F. La Mantia, P. Novak, P.G. Bruce, J. Am. Chem. Soc. 130 (2008) 3554–3559.
[7] J.C. Anderson, M. Schieber, J. Phys. Chem. Solids 25 (1964) 961–968.
[8] M. Brunel, F. de Bergevin, J. Phys. Chem. Solids 29 (1968) 163–169.
[9] D.E. Cox, G. Shirane, P.A. Flinn, S.L. Ruby, W.J. Takei, Phys. Rev. 132 (1963) 1547–1553.
[10] M. Wang, A. Navrotsky, J. Solid State Chem. 178 (2005) 1230–1240.
[11] M. Tabuchi, S. Tsutsui, C. Masquelier, R. Kanno, K. Ado, I. Matsubara, S. Nasu, H. Kageyama, J. Solid State Chem. 140 (1998) 159–167.
[12] M. Catti, M. Sommariva, R.M. Ibberson, J. Mater. Chem. 17 (2007) 1300–1307.
[13] E. Collongues, C.R. Acad, Sciences (Paris) 241 (1955) 1577–1580.
[14] J. Rodriguez-Carvajal, FULLPROF: a program for Rietveld refinement and pattern matching analysis, ⟨http://www.ill.eu/sites/fullprof/⟩.
[15] R.B. Von Dreele, J.D. Jorgensen, C.G. Windsor, J. Appl. Crystallogr. 15 (1982) 581–589.
[16] P. Thompson, D.E. Cox, J.B. Hastings, J. Appl. Crystallogr. 20 (1987) 79–83.
[17] R.D. Shannon, C.T. Prewitt, Acta Crystallogr. Sect. B 25 (1969) 925–946.
[18] T. Matsui, J.B. Wagner Jr, J. Nucl. Mater. 99 (1981) 213–221.
[19] L. Pauling, J. Am. Chem. Soc. 51 (1929) 1010–1026.